Mubarak ALANAZI[1]

# Control and monitoring of stand-alone hybrid renewable energy systems

ABSTRACT: Energy storage plays a critical role in stand-alone hybrid renewable energy systems, ensuring a stable and reliable power supply in rural areas disconnected from the electrical grid. This study integrates batteries and a backup diesel generator to maintain continuous energy availability. A computer-based monitoring and control unit is developed to optimize system performance, increase efficiency, and enhance sustainability. The experimental setup consists of photovoltaic (PV) panels, a diesel generator (DG), a battery bank (B), a charge controller, a DC/AC inverter, and a variable electrical load. The control unit, designed using LabView software, prevents battery over-discharge, thereby improving longevity and overall efficiency. It comprises voltage and current sensors connected to data acquisition cards (DAC) linked to a PC. The system features twelve 12 V PV panels, each rated at 75 W, supplying a total of 450 W. The experimental findings indicate that battery capacity declines significantly under high discharge currents, emphasizing the necessity of effective energy management strategies. The control unit continuously monitors system parameters and regulates the operation of the backup generator. When the battery's state of charge (SOC) drops to 35%, the system automatically disconnects the load and activates the DG, ensuring an uninterrupted power supply while prolonging the battery lifespan. These results highlight the importance of selecting suitable battery sizes and characteristics, considering both

✉ Corresponding Author: Mubarak Alanazi; e-mail: Alanazi3015@gmail.com, Anazi_m@rcjy.edu.sa

[1] Electrical Engineering Department, Jubail Industrial College, Royal Commission for Jubail & Yanbu, Saudi Arabia; ORCID iD: 0000-0001-9701-3761; e-mail: Alanazi3015@gmail.com, Anazi_m@rcjy.edu.sa

cost and load demands, to enhance the performance, reliability, and economic feasibility of hybrid renewable energy systems for off-grid applications.

# Nomenclature and abbreviations

| | | |
|---|---|---|
| AC | – | Alternative current [A] |
| Ah | – | Ampere hour |
| B | – | Battery |
| BC | – | Battery capacity [Ah] |
| COE | – | Cost of Energy [$/kWh] |
| $C_{nom}$ | – | The nominal capacity of the battery [Ah] |
| DC | – | Direct current [A] |
| DG | – | Diesel generator |
| DAC | – | Data acquisition card |
| $FF$ | – | Fill factor |
| HRES | – | Hybrid renewable energy systems |
| $I_b$ | – | Battery discharging current [A] |
| $I_n$ | – | Normalized discharging current [A.] |
| $I_{mp}$ | – | Maximum Power Curren [A] |
| $I_{mp}, V_{mp}$ | – | Maximum power point [A, V] |
| $I_{S.C}$ | – | Short – circuit current [A] |
| kWh | – | Kilo Watt hour |
| MPC | – | Model predictive control |
| MPPT | – | Maximum power point tracking |
| NPC | – | Net present cost |
| $N_L$ | – | Net load [W] |
| $N_r$ | – | Normalized factor |
| $P_b$ | – | Power required from the battery [W] |
| PC | – | Personal computer |
| $P_L$ | – | Power received by the cell surface [W] |
| $PV$ | – | Photovoltaic panels |
| $P_{max}$ | – | Maximum power [W] |
| RES | – | Renewable energy source |
| SOC | – | State of charge of the battery |
| $V_{mp}$ | – | Maximum power voltage [V] |
| $V_{O.C}$ | – | Open circuit voltage [V] |

$\eta_b$    –    Battery efficiency [%],
$\eta_{br\ ther}$–    brake thermal efficiency of diesel engine [%]
$\eta_{gen}$    –    efficiency of the generator [%]

# Introduction

Hybrid Renewable Energy Systems (HRES) can be configured as either off-grid or grid-connected systems. In grid-connected setups, they are generally used as fuel savers. These systems typically combine PV panels with battery storage and an auxiliary petrol generator and have been in operation across various applications for decades. Despite the research of different energy storage types for integration into HRES, storage batteries remain the leading technology for power storage in PV systems. Small and medium-sized PV-battery stand-alone systems are pervasive in distant applications, where batteries are subject to demanding conditions, including frequent charge/discharge cycles and long periods of deep discharge, which may significantly reduce their lifespan (Yap and Karri 2015). Lead-acid batteries are commonly utilized for energy storage in these systems. Selecting an appropriate battery bank size requires a thorough analysis of several factors, including the charge and discharge needs of the battery, load characteristics, output from PV or alternative energy sources, operating temperatures, and the efficiency of the charger and other system components (Makbul et al. 2015). In their simulation study of a hybrid PV/wind turbine system, they suggested that maintaining the battery's SOC between 30% and 100% can extend its lifespan to 12 years. For HRES to be a technically reliable and cost-effective solution, both the system configuration and the control strategy are crucial. An intelligent control strategy can not only prolong the system's operational lifespan but also optimize the efficiency of the diesel generator, ensuring it operates within its most efficient load range (Datta et al. 2009; Shin et al. 2015; Maleki and Pourfayaz 2015; Nfah et al. 2007).

# 1. Hybrid renewable energy systems

Hybrid Renewable Energy Systems represent a sophisticated approach to solving power supply challenges in remote locations by integrating various energy generation components. These systems typically combine photovoltaic power supplies with other renewable energy sources (RES) and a diesel generator (DG), creating a versatile solution for remote sites (Thirunavukkarasu et al. 2020; Farahat et al. 2019). The primary function of stand-alone HRES is to provide reliable electricity to remote telecommunication stations, mountain huts, private

houses, isolated farms, and villages, showcasing their versatility across diverse climates and applications (Abd-Elaziz et al. 2021; Hansen et al. 2001). HRES configurations often include a combination of PV with diesel generators and battery storage, known as *PV*/Diesel/Battery systems, or *PV* with wind and battery storage, referred to as *PV*/Wind/Battery systems. These configurations have been successfully deployed in various environmental conditions, emphasizing *PV* as a prevalent and efficient solar energy source. Such optimization was explored in a case study set in Malaysian weather conditions, focusing on maximizing efficiency and energy retention (Shen 2009). The standalone photovoltaic (SPV) system configuration, illustrated in Figure 1, includes a solar array, an MPPT controller, a battery (B), an inverter, and electrical loads designed to ensure maximum power extraction and battery protection.
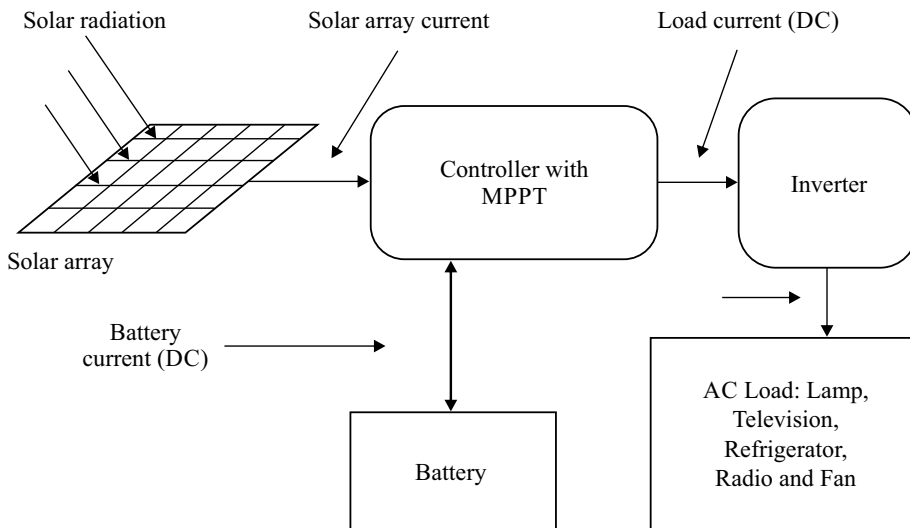


Fig. 1. Stand-alone PV- battery system

Rys. 1. Samodzielny system baterii fotowoltaicznych

The global shift towards clean, renewable solar energy, particularly for replacing oil-produced energy, is gaining momentum. In Saudi Arabia, a techno-economic study utilized long-term solar radiation data from Dhahran to evaluate the effectiveness of hybrid PV-DG-B systems, highlighting the region's high solar radiation as an asset for solar *PV* deployment (Shaahid et al. 2008). Similarly, (Abdelmjid 2020) conducted a study in Morocco, assessing the feasibility of HRES to power domestic loads across eight cities, thereby demonstrating the system's adaptability to different regional energy requirements. Datta et al. 2010; introduced a fuzzy-based frequency-control method tailored for large, isolated utility-connected PV-DG systems. This method addresses frequency deviations due to fluctuating PV power and uses an Energy Storage System (ESS) to smooth out the PV output power fluctuations. Figure 2 shows the PV- D - B system. The economic impact of integrating HRES is significant, with batteries often

constituting over 40% of the system's lifecycle costs. Extending battery life through optimal charging and discharging is crucial, (El-Hefnawi 1998; Zhang et al. 2017) proposed a distributed utility engineering micro-grid topology, which enhancing the efficiency and reliability of HRES.

The National Renewable Energy Laboratory (NREL) demonstrated the scalability of these systems by commissioning a 430 kW PV system with inverters, designed for easy expansion up to 1 MW (Gevorgian et al. 2022). Optimization studies have shown that configurations involving *PV*, wind turbines (WT), B, and DG offer a cost-effective solution, achieving a cost of energy (COE) of \$0.2109 per kWh (Belboul et al. 2024). Technical, economic, and environmental assessments continue to push the boundaries of HRES technology. Studies by (Chen et al. 2023; Habib et al. 2019; Ganthia et al. 2022) along with discussions led by (Samia et al. 2024; Mohanty et al. 2015). These studies explored different control strategies for hybrid PV/DG/B systems, proving that these configurations could sustain energy supply over extended periods under varying solar conditions. Additionally, the development of micro-grid topologies and energy management strategies that incorporate battery capacity prediction and renewable energy power generation forecasting are critical for realizing the full potential of HRES. These advancements are crucial for enhancing the economic viability and environmental sustainability of HRES, making them a pivotal solution in the transition toward a more sustainable global energy system.

## 1.1. Hybrid renewable energy system characteristics

Hybrid Renewable Energy Systems crucially rely on the performance characteristics of their components, with *PV* modules playing a pivotal role. The performance of *PV* modules is primarily determined by three classical parameters: short-circuit current ($I_{S.C}$), open-circuit voltage ($V_{O.C}$), and the maximum power point ($I_{mp}$; $V_{mp}$). At the maximum power point, the power output from a *PV* cell reaches its peak, which is critical for optimizing the energy efficiency of the system. This data is fundamental for constructing a basic model of the module to test power converters; however, a more detailed model would require additional parameters for higher accuracy (Abed et al. 2018).

Another essential parameter in evaluating *PV* module performance is the fill factor (*FF*). The fill factor is a measure of how well a cell's semiconductor junction can harness the carriers generated by light, effectively describing how the curve fills the rectangle defined by ($V_{O.C}$), ($I_{S.C}$) and can be calculated using the Equation:

$$FF = V_{mpp}I_{mpp} / V_{O.C}I_{S.C} \qquad (1)$$

After a simple manipulation the following Equation results:

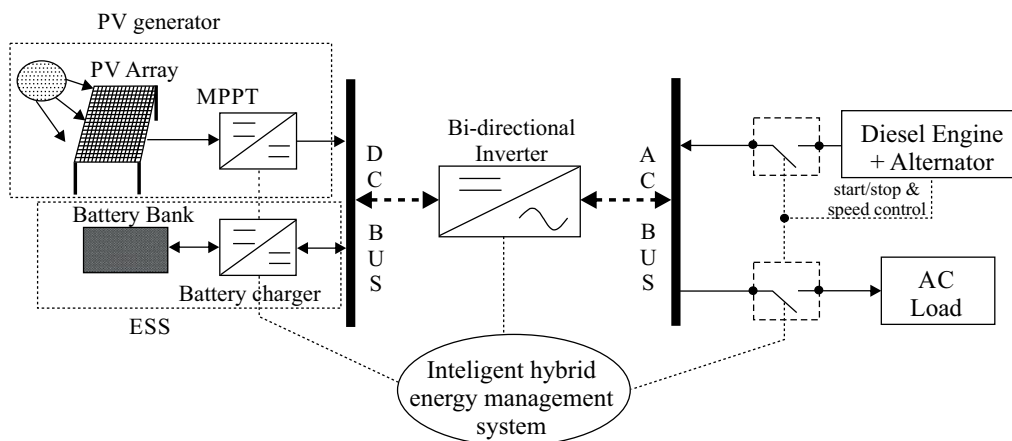$$V_{O.C}I_{S.C} \ FF = V_{mpp}I_{mpp} = P_{max} \qquad (2)$$

Fig. 2. Parallel PV–diesel–battery system

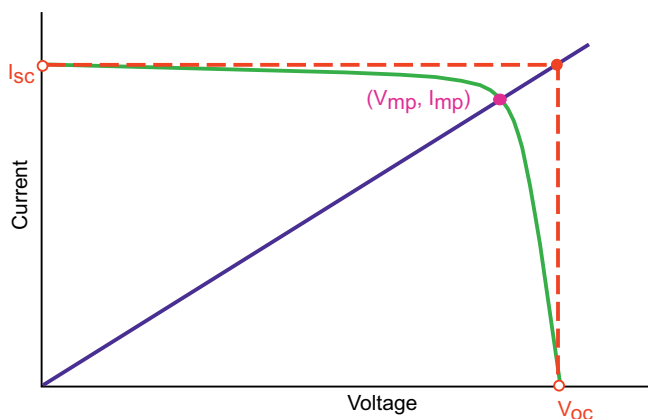Rys. 2. Równoległy układ PV–diesel–bateria



Fig. 3. Photovoltaic module characteristics

Rys. 3. Charakterystyka modułu fotowoltaicznego

The efficiency of the cell ($\eta$) is defined as the ratio of the maximum output power to the solar power received by the cell surface ($P_L$):

$$\eta = V_{mpp}\ I_{mpp}\ /\ P_L \qquad (3)$$

## 1.2. Storage battery

Lead-acid and nickel-cadmium batteries, the most common, are used with *PV* systems. These are available in different forms, such as flooded-vented and valve-regulated in absorbed or gel form. For this research, gel batteries were selected due to their semi-solid electrolyte, which prevents spillage and enhances safety and maintenance. Commonly, batteries are configured in blocks of 2-volt cells, with 12-volt and 6-volt configurations being most prevalent (Duryea et al. 1999). Battery capacity is a critical performance metric that specifies the amount of energy a battery can store, measured in ampere-hours [Ah]. The battery's discharge current ($I$) can be calculated by dividing the power required from the battery ($P_b$) by the voltage ($V_1$) and the percentage of battery capacity utilized:

$$I = P_b / V_1 \tag{4}$$

Normalized factor ($N_r$) is calculated by dividing battery capacity ($B_c$) with nominal capacity ($C_{nom}$) of the battery [Ah]:

$$N_r = Bc / C_{nom} \tag{5}$$

where:

$C_{nom}$ – the nominal capacity of the battery [Ah],
$B_c$ – the battery capacity [Ah].

Using the normalization factor $N_r$, the normalized current ($In$) is calculated;

$$I_n = I \cdot N_r \tag{6}$$

where:
$I$ – discharge current [A].

By interpolation, the relevant percentage capacity used to discharge current ($I$) for a one-hour period is computed.

In renewable energy systems, solar batteries are charged and discharged on a daily basis. When solar radiation falls owing to weather conditions, the *PV* array provides less energy, lowering the battery's SOC (Duryea et al. 1999). When the SOC is low, the system attempts to match the load requirement, resulting in daily cycles around the deep discharge. A sophisticated management system could monitor the SOC and gradually decrease the energy drawn from the battery to prevent continuous operation at a low state of charge, thereby enhancing battery life and system reliability. Low SOC can significantly shorten the battery's lifespan, and the battery's capacity is not a viable solution for the peak demand of the worst season (Zhou et al. 2010).

Ah-efficiency, a crucial performance parameter, is determined by integrating the charging and discharging currents over time. It is calculated as follows:

$$\eta_{Ah} = \frac{\int_0^t I_{dchg} \, dt}{\int_0^t I_{chg} \, dt} \tag{7}$$

where:

$\eta_{Ah}$   –   Ah-efficiency [%],
$I_{dchg}$   –   discharge current [Ah],
$I_{chg}$   –   charge current [Ah].

This formula provides a measure of the battery's ability to efficiently convert stored energy back into electrical power, reflecting the effectiveness of the battery management system.

## 1.3. Charge controller

Various types of solar charge controllers are available, with and without a Liquid Crystal Display (LCD). In this research, we utilize a charge controller equipped with an LCD that displays the accurate SOC of the battery in percentage. The output power of a *PV* system fluctuates based on weather conditions, seasonal changes, and geographic location. The charge controller is essential for regulating these fluctuations, ensuring that the generated power is either directly supplied to the user or to the utility efficiently and safely.

1. Required controller protective functions:
2. Protection against reverse polarity of solar modules
3. Protection against reverse polarity of connected battery:
4. Protection against overcharging.
5. Open circuit-proof during operation without battery or consumer.
6. Overvoltage and undervoltage protection.
7. Excess temperature protection
8. Overload protection at load output.

## 1.4. Diesel engine generator unit

The diesel engine generator unit was added to ensure a continuous power supply and compensate for the intermittent nature of photovoltaic in HRES. The following two cases should be considered to determine the rated capacity of the engine generator to be installed.

1. If the diesel engine generator unit is directly connected to a load, then the rated capacity of the generator must be at least equal to the maximum load and

2. If the diesel engine generator is used as a battery charger, then the current produced by the generator should be less than $\dfrac{C_{Ah}}{charging\ time} A$, where $C_{Ah}$ – the ampere-hour capacity of the battery. The overall efficiency of diesel generators is given by (Deshmukh et al. 2008).

$$\eta_{overall} = \eta_{br.\ ther.} \cdot \eta_{gen} \tag{8}$$

where:

$\eta_{br.ther.}$    –    brake thermal efficiency of diesel engine [%],
$\eta_{gen}$     –    efficiency of the generator [%].

If the generator is operated at 70–90% of full load then it is economical (Bilal et al 2012). In the absence of peak demand, diesel generators are normally used to meet load requirements and charge batteries.

## 1.5. Inverter

In a solar photovoltaic system, solar cells are used to convert light into DC electricity. This DC electricity is generated when solar radiation strikes the *PV* module. Consequently, a storage device is needed to supply power to loads that require electricity at night or during periods of low radiation. For appliances that operate on AC, an inverter is essential to convert DC into AC. Power delivered by the inverter to meet the demand can be described by the following Equation (Bilal et al 2012):

$$P_{in} = \frac{P_{out}}{\eta_{in}} \tag{9}$$

where:

$P_{in}$    –    represents DC input power in watts,
$P_{out}$   –    AC output power in watts,
$\eta_{in}$    –    Inverter efficiency

$P_{out}$ is the output AC power from the conditioning unit (W) and the inverter efficiency, which is usually provided by the manufacturer in percentage. This data is crucial for determining how efficiently the inverter converts stored DC power into usable AC power, which affects the overall efficiency and utility of the solar PV system (Mertens et al. 2014).

## 1.6. Control scheme

The control scheme in HRES is crucial for efficiently coordinating and dispatching the available energy. The primary objective of system operation control is to utilize the energy from each component efficiently, aligning with key factors such as economic operation, environmental impact, reliability of supply, and quality of the delivered energy. In all system configurations, the agreed strategy prioritizes utilizing the output from renewable energy converters (e.g., photovoltaic systems) to meet the load requirements. When renewable energy output is insufficient, various strategies are implemented to manage the deficit. One approach is to use the energy storage system to meet the immediate demand (defined as net load) first, and the diesel generator supplies any remaining requirements. Conversely, another strategy suggests drawing the net load primarily from the diesel generator, with the storage system providing any additional required energy (Castañeda et al. 2013). These strategies significantly influence the operational lifetime of system components and, consequently, the costs associated with energy generation.

Unlike renewable sources, diesel generators and storage units are the leading controllable energy suppliers within HRES. Therefore, operation control must effectively exploit its operational characteristics to meet the expectations placed on the supply systems. For renewable converters, the standard configurations include systems without storage, which rely on an auxiliary diesel engine driving a generator, and systems with battery storage. The operational modes of the diesel engine in renewable energy systems can vary, including continuous operation, start/stop operation, and serving as an uninterrupted power supply (Ibrahim 2002). The integration of battery storage in decentralized HRES serves as an energy buffer, enhancing the level of renewable energy usability and improving system energy availability.

Furthermore, battery storage helps to stabilize fluctuations in renewable sources and can optimize the on/off frequency and fuel consumption of the diesel generator. The strategies for utilizing diesel power to charge the battery and managing the use of battery storage to meet net-load demands are areas of particular interest and debate. Various fundamental concepts and strategies to optimize system operation control include battery cyclic charge strategy, rated-power strategy, and periodic-full-charge strategy (Castañeda et al. 2013). Regarding diesel generator usage, four strategies are prevalent: load-following, using diesel exclusively to charge the battery, frugal discharge, and employing diesel solely for battery charging.

# 2. Development of an advanced control concept

The development of an advanced operational control concept is centered around a rule-based system. This approach focuses on strategic energy management and the efficient utilization of system components. The primary objectives of this advanced operational control are to minimize energy production costs through optimal scheduling of power units (such as diesel generators and batteries) and by implementing regimes that mitigate the degradation mechanisms of the battery bank.

## 2.1. Operating constraints module

*PV* inverters, critical components in this system, are equipped with security features that protect against dangerous conditions like high currents and voltages. They also include functions that safeguard *PV* modules during periods of high insolation with minimal or no load. They also prevent short-circuiting while maintaining maximum power point tracking (MPPT) to protect the costly *PV* modules. Key aspects of the control concept focus on the energy management of the diesel engine and the battery storage, with specific constraints including:

✦ Minimum allowable diesel loading ratio: The loading ratio and the idling conditions of the diesel engine are limited. The engine manufacturers recommend that the minimum loading ratio be between 40% and 50% of the engine's nominal power.

✦ Critical power: A critical power criterion was implemented to ensure efficient distribution of net load ($N_L$) between the battery and diesel generator. According to this criterion, rational use of battery capacity is ensured if its value is correctly selected. Moreover, the diesel's on/off frequency is minimized.

✦ Minimum allowed state of charge: This constraint directly influences the battery's cycle life. Therefore, recommendations are made to stop the battery discharge at a predefined state of charge, usually at 30% of the actual battery capacity. In addition to the SOC, the end-of--charge and discharge voltages are also important for battery durability.

In renewable systems with either diesel generators or battery storage, there is no degree of freedom if the load is to be covered. In systems with renewable/battery, the battery either supplies the shortfall or absorbs the surplus energy of the renewable.

IF     $N_L < 0$     Then charge battery (if possible),
IF     $N_L > 0$     Then discharge battery (if possible),

In systems with renewable/diesel, the diesel supplies the shortfall of renewable power in meeting the load.

IF     $N_L < 0$     Then stop diesel generator,
IF     $N_L > 0$     Then start diesel generator.

## 2.2. General control functions

The general control functions of this concept include:
- ✦ Decisions for switching the diesel generator on/off and defining its operating point.
- ✦ Charge/discharge decisions for the battery.
- ✦ Strategies to decelerate battery degradation mechanisms.
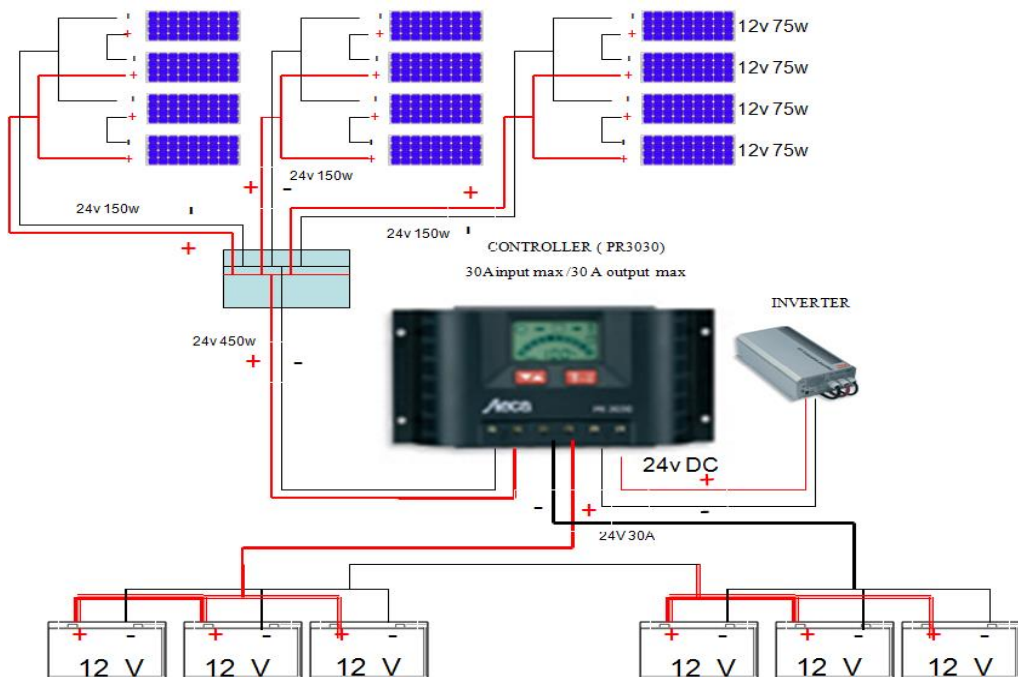- ✦ Parallel operation of diesel and battery for enhanced energy availability.

# 3. The system configuration

The system comprises an array of components, including *PV* modules, batteries, a charge controller, an inverter, a backup diesel generator, and a variable load. The system›s performance is monitored and controlled through a control panel equipped with a USB data acquisition card connected to a PC. This setup also includes various signal conditioning devices and transducers, all managed through a custom-developed LabVIEW software program. The technical specifications of the used components are:
- ✦ 12 PV modules, each rated at 75 watts.
- ✦ 6 batteries, each with a capacity of 100 Ah at 12V.
- ✦ Charge controller: controls power flow from PV modules to batteries and loads.
- ✦ The inverter converts DC to AC for usage with AC loads.
- ✦ The diesel generator provides 2.2 kW of rated power as backup energy.
- ✦ Manual variable load: 50–450 watts.
- ✦ Control panel: designed for system management.
- ✦ The PC is IBM-compatible and includes LABVIEW software for logging, display, and control.

The system›s performance is continuously monitored and regulated via a control panel, which incorporates a USB DAC connected to a PC. Several transducers and signal conditioning devices complement this setup, all managed through a custom-developed LABVIEW software program. The control panel is equipped with three transducers designed to measure currents from the *PV* modules, batteries, and inverter. The currents of the *PV*, batteries, and inverter, along with the battery SOC, are diligently monitored, displayed, and recorded. The control scheme has been meticulously calibrated to accommodate varying levels of irradiation and load, ensuring optimal performance. Fluctuations in *PV* power can lead to frequency deviations within power utilities, mainly when system penetration is extensive. Batteries in *PV* systems exhibit distinct performance characteristics. Notably, the lifecycle costs of these batteries are substantial, sometimes accounting for more than 40% of the total system costs (Abed et al. 2018). The solar charge controller, a critical component of the experimental setup, manages the power flow effectively. The connection panel of the Model PR3030 solar charge controller receives power

from the *PV* modules, supplying the immediate load demands and utilizing excess energy to charge the batteries. In scenarios where the load demand exceeds the *PV* output, the controller draws power from the batteries to mitigate any shortages.

The charge controller safeguards the batteries from excessive discharging. In the present configuration, if the battery›s SOC falls below a predetermined level, the load is disconnected to prevent deep discharge. The control panel in this setup can override these SOC thresholds. Specifically, it disconnects the load from the PV and battery system when the SOC is less than or equal to 35% and triggers the start of the diesel-powered generator. The system utilizes an IBM-compatible PC equipped with a display and multiple USB connectors. These connectors link the PC to the control panel›s Data Acquisition Card. The PC boasts adequate storage capacity for data collection and is adept at receiving and processing operational data promptly. The LABVIEW software suite, which is used to generate the operational code for this research, interfaces with the DAC. These parameters are presented on the monitor in an accessible format, using charts and numerical values to display current and voltage data.

The data processed by the LABVIEW software informs decisions about when to initiate generator operations, which are then relayed to the control panel. Following instructions from the PC, the DAC card transmits on/off commands to the system. Figure 4 shows the primary connections of the system components.



Fig. 4. The main connections of the system components

Rys. 4. Główne połączenia elementów systemu

# 4. Control strategy

The control approach for HRES comprises several critical components:

◆ Data management: Utilizing a PC for data logging, processing, displaying, and controlling processes.
◆ Collecting available signals and status data using transducers and switches.
◆ Data Acquisition: Use a data acquisition system to connect the PC and signals.
◆ Real-time display: Graphical representation of real-time data for quick understanding and response.
◆ Data analysis and control: Using real-time data to generate switching signals.
◆ Performance analysis: Analyze HRES performance based on logged data.

This DAC unit is managed through a specially developed interface using LABVIEW software. It converts analog signals that represent system parameters into digital data, which is then sent to the PC. Here, the dedicated LABVIEW program displays the data, stores it on the PC disk, and processes it further for operational decision-making. This processed data informs decisions regarding the operation of the diesel-based generator, directing the DAC card in the control panel to issue ON/OFF instructions to the system. The flow chart detailing this control strategy is depicted in Figure 5.
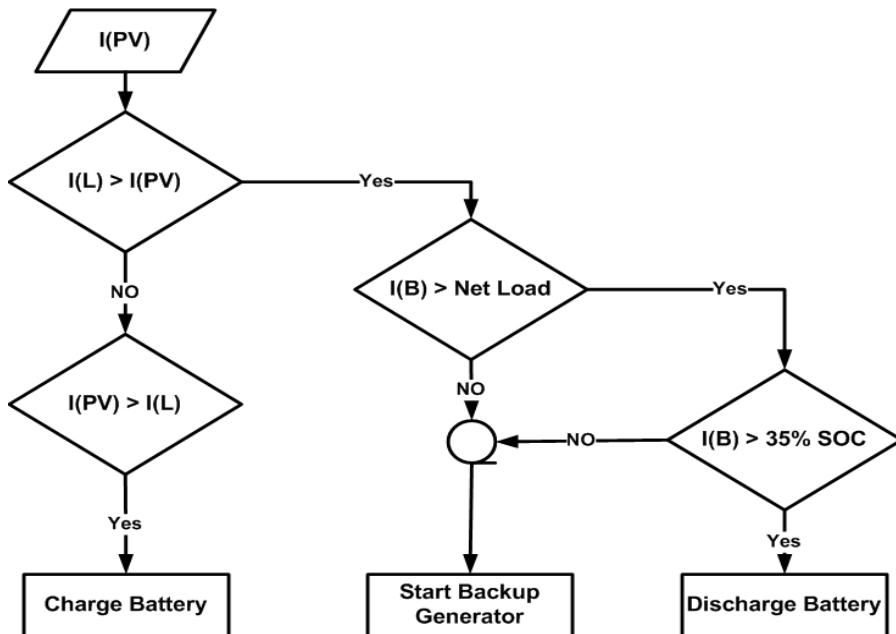


Fig. 5. Flow chart of the control strategy

Rys. 5. Schemat blokowy strategii sterowania

## 4.1. Battery state of charge

The state of charge of the battery is defined as the ratio of the difference between nominal capacity and charge balance, divided by the nominal capacity (Abed et al. 2018). Given that daily energy demand remains relatively constant, a decrease in solar radiation due to weather conditions results in a reduced energy supply from the *PV* array, thereby lowering the SOC. When the SOC is low, the system may still attempt to meet the demand, causing the battery to cycle around the deep discharge threshold. An advanced management system is crucial for monitoring the SOC and appropriately adjusting the energy drawn from the battery. Deep discharge protection (DDP) is typically implemented by detecting the battery voltage, which does not precisely reflect the state of charge. During the winter months, the battery may have a low SOC. Severe low SOC situations might substantially shorten the battery's life. One of the main objectives of the proposed battery management system is to correctly assess the SOC and use this information to reduce lengthy periods of low SOC, hence increasing battery life and system reliability.

## 4.2. Effect of battery state of charge

The current study thoroughly investigated the effect of the battery state of charge on the system's capacity to satisfy demand. The power delivered to various loads was measured at various charge levels. The SOC [%] did not have a substantial effect on battery output. The SOC of batteries was calculated by integrating or summing the battery output current (Ah) multiplied by the discharge duration. Initially, batteries were charged entirely (i.e., 100% SOC), then drained to 35% SOC with a fixed 400-watt load, and the Ah was integrated using Equation (10). The summing approach was used to calculate battery capacity at different SOC levels ranging from 100% to 40%, with each drained down to 35% SOC. Battery state of charge could be calculated using Equation (10):

$$SOC = \left[ \frac{C_{nom} - Q_{Bat}}{C_{nom}} \right]$$
(10)

where:

$$Q_{Bat} = \int_t I \, dt$$

Cnom  –  the nominal capacity of the battery [Ah],
$Q_{Bat}$  –  the AH-balance (i.e. net AH discharged since the last full state of charge),
$I$  –  the main reaction current [A].

In the current system setup, where current is measured every two seconds, the battery capacity was calculated using:

$$Battery\ Capacity = \sum_{soc\ 35\%}^{soc\ 100\%} I \,.\Delta t \tag{11}$$

where:

$\Delta t = 2$ sec.

The first task of the control system is to monitor the SOC of the batteries, ensuring that it recognizes when the SOC has decreased to the level of 35%. At this point, the system automatically instructs the operator to switch on the backup generator. This automated response is crucial for maintaining a continuous power supply and protecting the batteries from deeper discharge levels that could shorten their lifespan. The second task facilitated by this test is to enable the system to restart at any battery SOC as specified by the battery charge controller. This feature is significant after the system has been shut down for service or other reasons. The software uses the measured SOC to assess the available battery capacity and calculate the actual ampere-hours [Ah] withdrawn. This calculation is vital for accurately determining when the SOC has reached 35%, a threshold at which the backup generator needs to be started to support the system's load.

## 4.3. Effect of load on battery capacity

System measurements were conducted under fixed and variable loads to evaluate the performance of the system and understand how actual system conditions affect battery capacity. It was observed during these tests that at lower loads (discharge currents), the SOC readings on the charge controller were higher than those displayed on the program screen, except at a load of 400 Watts, where the results matched. This discrepancy suggested that battery capacity varies with different discharge currents. To further explore this phenomenon, a series of tests were performed where the summation of the discharged current (actual Ah) was calculated for batteries discharging from 100% SOC down to 35% SOC, using various fixed loads. The findings indicated a decrease in battery useful capacity at higher discharge currents. For instance, at a 400 W load, the battery capacity was approximately 66 Ah, compared to the typical capacity of 100 Ah/20 hr. This highlights poor battery performance when discharged at higher rates and underscores the importance of accurately detecting SOC for optimal system management. A novel approach is proposed to enhance SOC detection in the proposed systems. This method involves using the IV curves of the batteries to determine the SOC without relying on SOC measurements from the charge controller, which is particularly useful when the system is restarted. To validate this approach, a series of tests were conducted where the voltage values of the batteries were recorded at different discharge currents and SOCs.

# 5. Results and discussions

This section summarizes the results of several months of data collecting, focusing on system performance under various environmental circumstances.

## 5.1. Case 1: PV output current exceeds load

Figure 6 depicts the *PV* output current on a day with frequent cloud cover and periods of sunshine, with a constant demand of 200 watts. During periods of sunshine, the *PV* current was sufficient not only to supply the load's inverter current but also to charge the battery, as indicated by a negative battery current. However, during cloudy periods, the *PV* current was insufficient, necessitating the extraction of the required current from the battery. This resulted in a periodic decline in battery voltage, as shown in the graph.
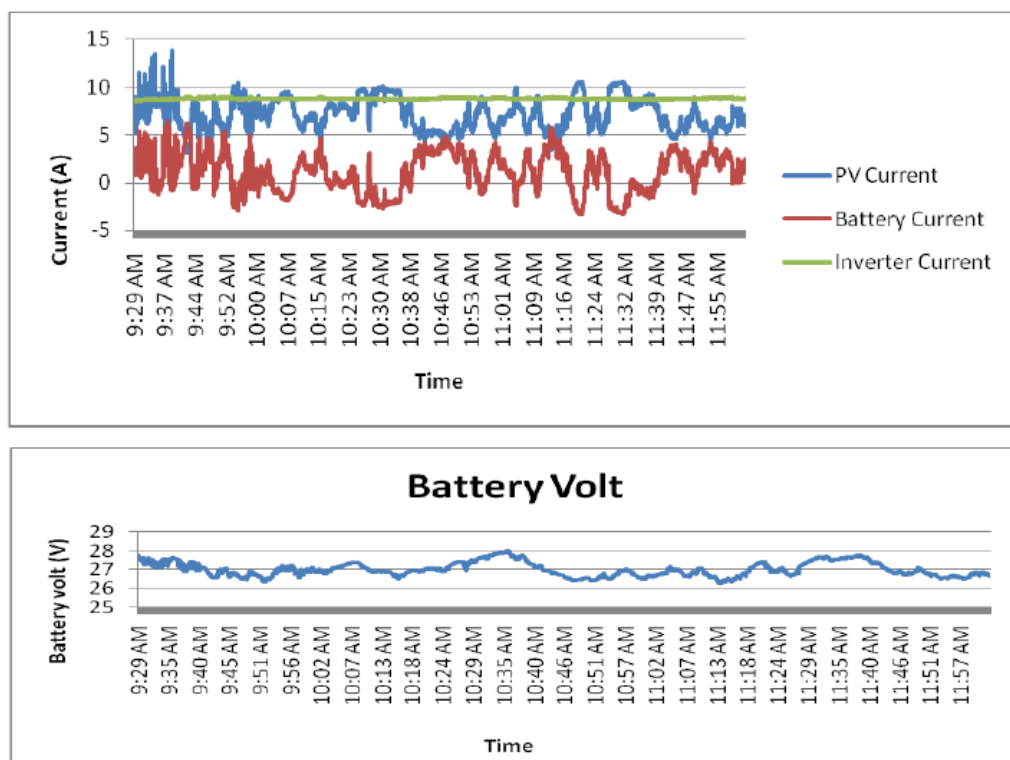


Fig. 6. Collected data of a day frequent clouds and frequent sunshine at load 200 W

Rys. 6. Zebrane dane z dnia, częste zachmurzenie i częste nasłonecznienie przy obciążeniu 200 W

## 5.2. Case two: *PV* and battery feeding the load
### (*PV* output current exceeds battery current)

In this case, the *PV* output current was insufficient to supply the load fully, necessitating the use of batteries to solve the shortage. As a result, the *PV* current was consistently lower than the load current, forcing the batteries to remain in a constant state of discharge, as shown by positive current flow. Under these conditions, the battery voltage gradually dropped as the batteries were continually drawn upon. The rate of discharge varies according to the load current. Figure 7 depicts the system performance and battery voltage when the batteries were discharged at a rate of about 5.5 amps under a 400-watt load. The initial SOC for this run was 75%.
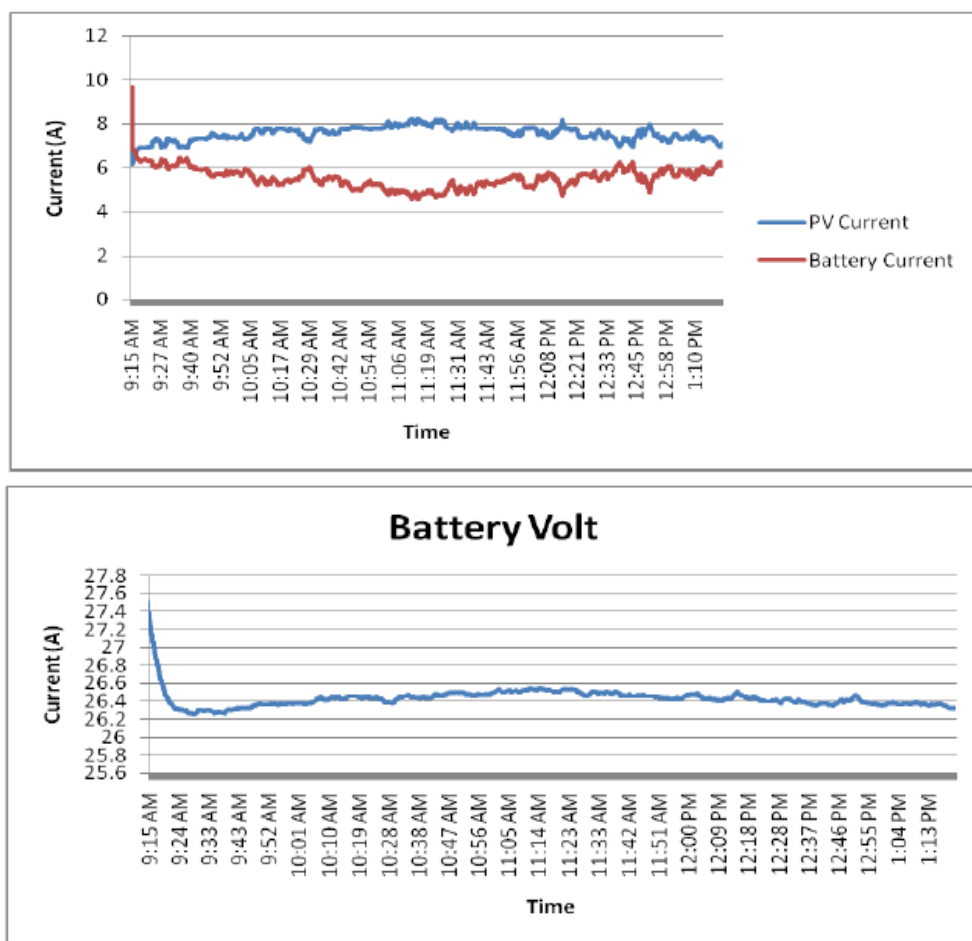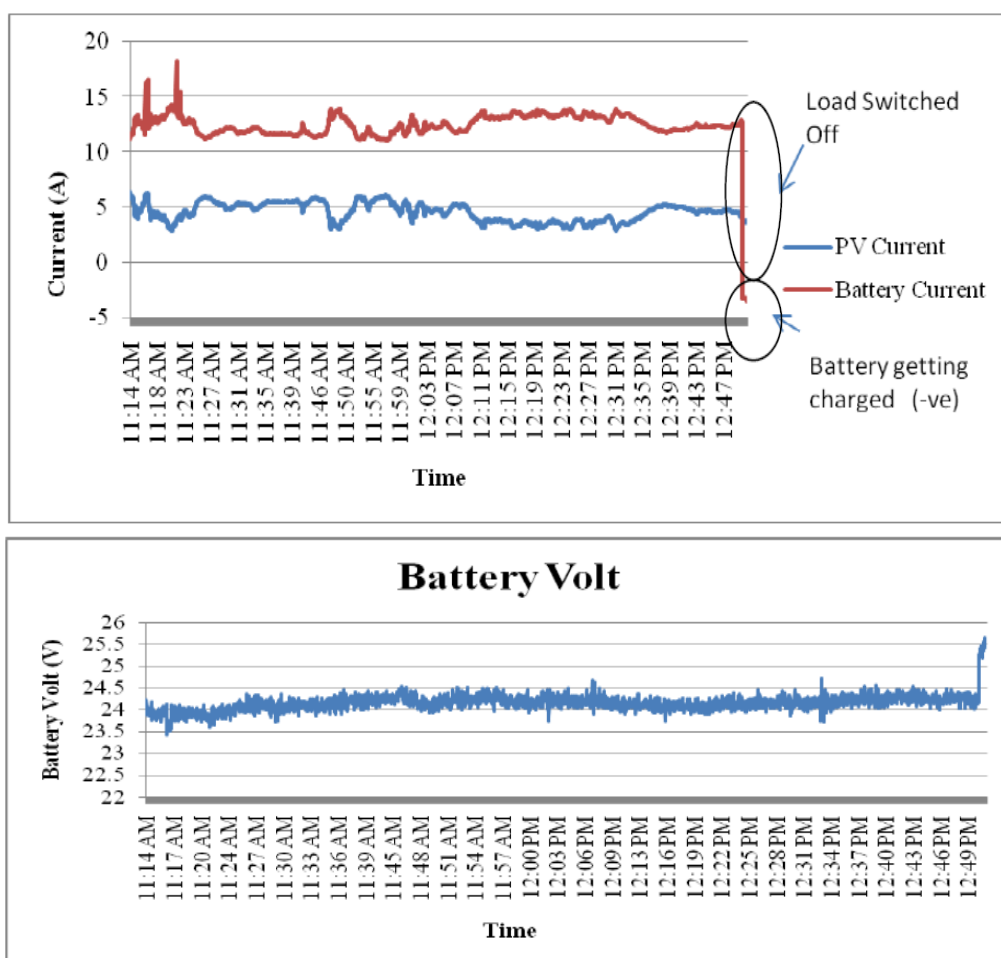


Fig. 7. System performance and battery voltage when batteries were discharged at rate around 5.5 A at load 400 W

Rys. 7. Wydajność systemu i napięcie baterii przy rozładowywaniu baterii z szybkością około 5,5 A przy obciążeniu 400 W

## 5.3. Case 3: *PV* and battery power supply the load
### (*PV* output current < battery current)

In this circumstance, the *PV* output current was significantly low, and the load needed to be met on its own was unable to be met. As a result, the batteries were required to provide the majority of the load current. When the load was eventually turned off, the battery current decreased to zero, and the batteries began to take the available *PV* current to recharge. Figure 8 depicts the system's performance and battery voltage when the batteries were discharged at a high rate of approximately 12.5 amps. Notably, as the load was turned off, the batteries began to charge utilizing the *PV* current.



Fig. 8. System performance and battery voltage when batteries were discharged at rate around 12.5 amps

Rys. 8. Wydajność systemu i napięcie akumulatorów rozładowywanych z natężeniem około 12,5 A

Figure 9 displays a similar scenario in which the battery discharge rates ranged from about 20 to 8 A. The *PV* current fluctuated dramatically and was less than half of the load current, resulting in irregular discharge patterns and fluctuating battery voltages.
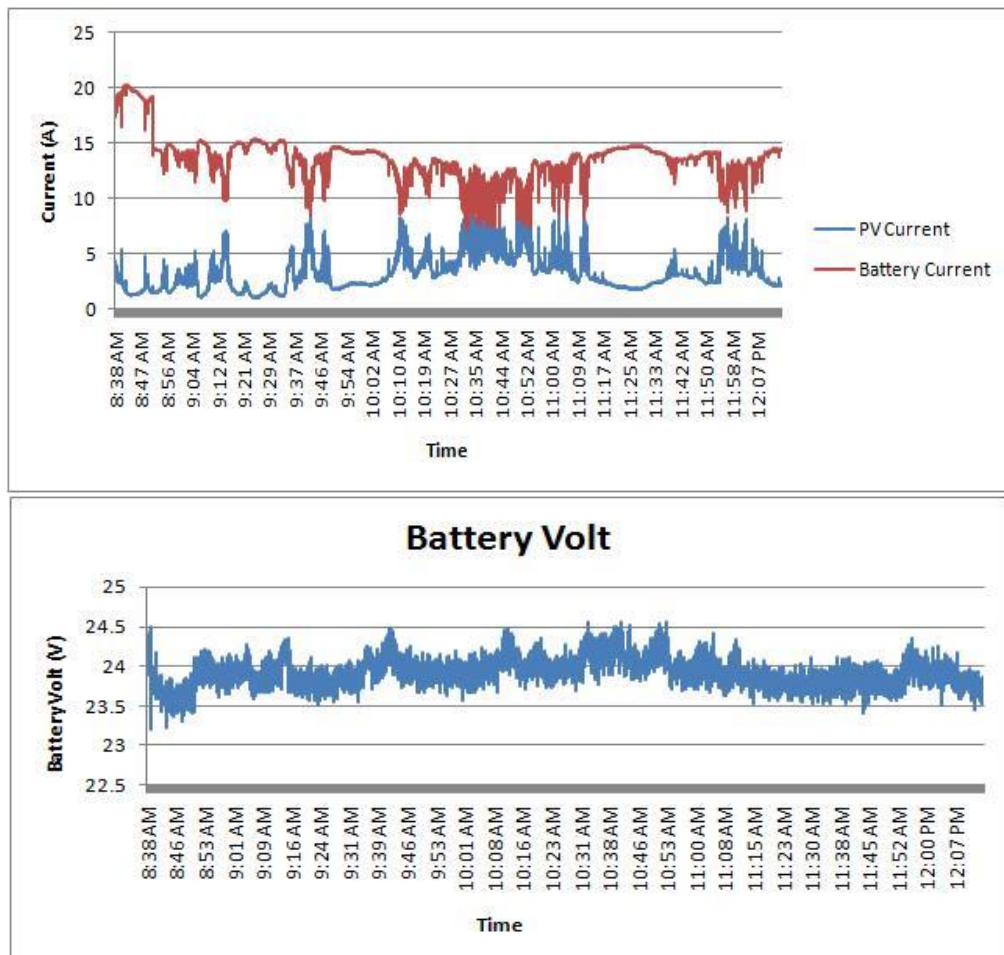


Fig. 9. System performance and battery voltage when batteries discharged at rates ranging from around 20 to 8 amps

Rys. 9. Wydajność systemu i napięcie akumulatorów rozładowywanych z natężeniem od około 20 do 8 amperów

The system performance after sunset, when *PV* current decreases to zero, is shown in Figure 10. The test began with the batteries at 100% state of charge. Due to continuous high-rate discharge, the battery SOC decreased to 35% within about 3 hours, forcing the activation of the backup generator.
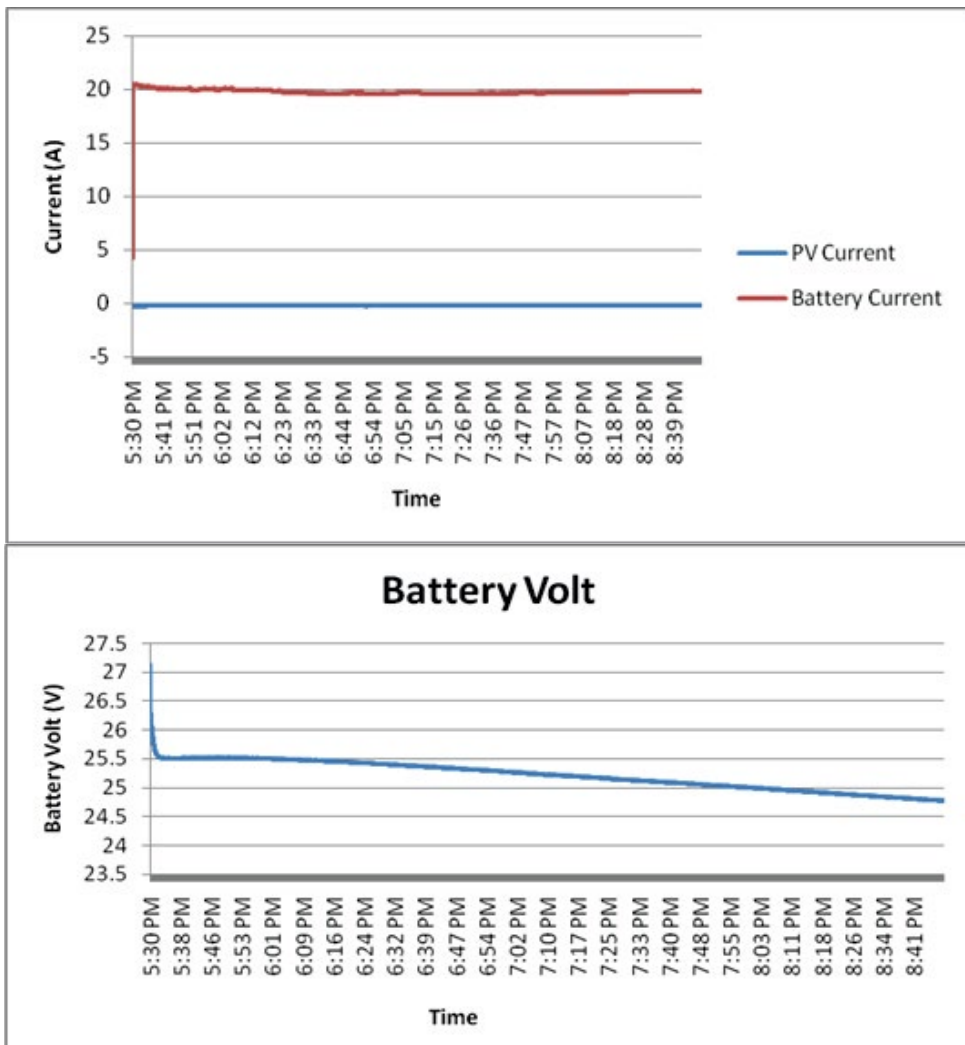
Fig. 10. System performance after sunset $PV = 0$

Rys. 10. Wydajność systemu po zachodzie słońca $PV = 0$

## 5.4. Case four: hybrid supply from *PV* and batteries

This situation reflects a combination of events observed in Situation Two and Case Three, where the power supply to the load alternates between *PV* panels and batteries based on the availability of solar radiation. Initially, when enough sunlight was available, the *PV* panels could handle large quantities of the load. Figure 11 depicts the system's performance at sunrise when solar radiation was sufficient to supply the majority of the load current via *PV*. As the intensity of

the sunlight dropped, the batteries took over, delivering the vast majority of the load current. This dynamic interplay demonstrates the system's capacity to respond to changing sunlight conditions throughout the day. Figure 12 shows the variation in battery voltage under a steady full load of 450 watts and dramatically fluctuating *PV* current. When the *PV* current is insufficient to satisfy the load demand, the battery supplements the *PV*, causing a fall in battery voltage due to increasing discharge. The battery voltage response under a lighter, continuous load of 200 watts on a cloudy day with varying *PV* current is shown in Figure 13. In circumstances where the *PV* current is insufficient to cover the load; the battery assists in powering the load, which results to
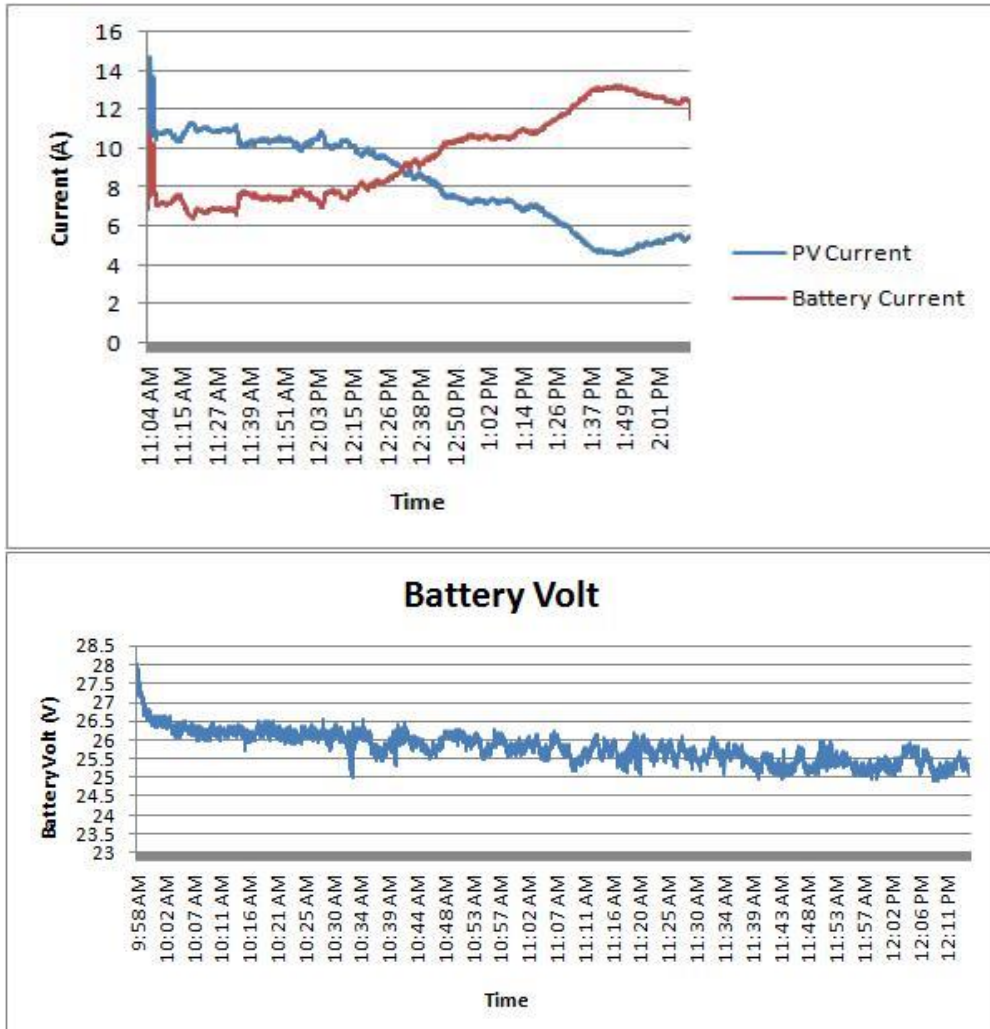


Fig. 11. System performance at the sun rise
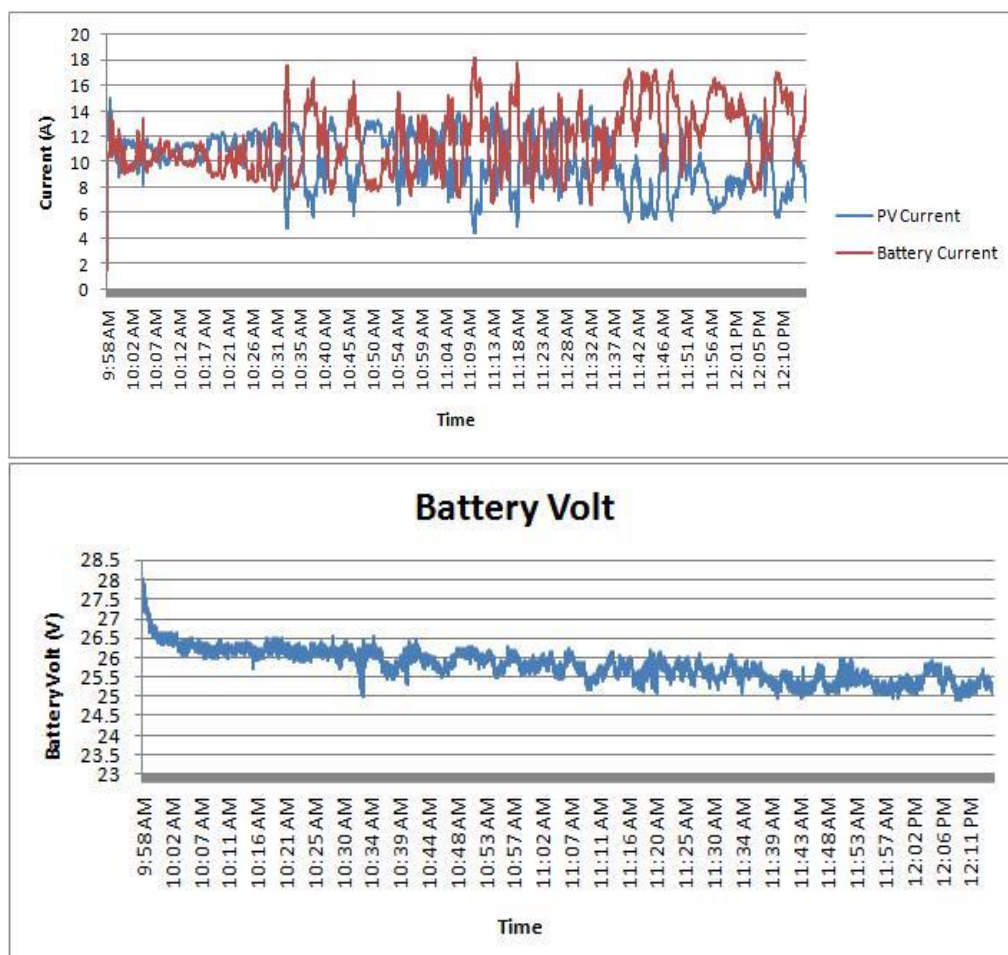
Rys. 11. Wydajność systemu o wschodzie słońca

44

Fig. 12. System performance and battery voltage when subjected to a constant load (at full load 450 watt)

Rys. 12. Wydajność systemu i napięcie akumulatora poddane stałemu obciążeniu (przy pełnym obciążeniu 450 watów)

a drop in battery voltage. When the *PV* current exceeds the load demand, the excess energy is directed toward charging the battery, increasing battery voltage.

Figure 14 depicts the system›s minimal voltage fluctuations during rare instances of sunshine. At the start of this measurement, the battery›s SOC was 98%, with a constant load of 200 watts. System performance on a cloudy day, characterized by fluctuating sunshine levels, is illustrated in Figure 15. This run began with the batteries at a SOC of 74%. As the batteries were continuously discharged, their SOC eventually decreased to 35%. At this critical threshold, the inverter was turned off, and the backup generator was activated to maintain the system›s power supply.
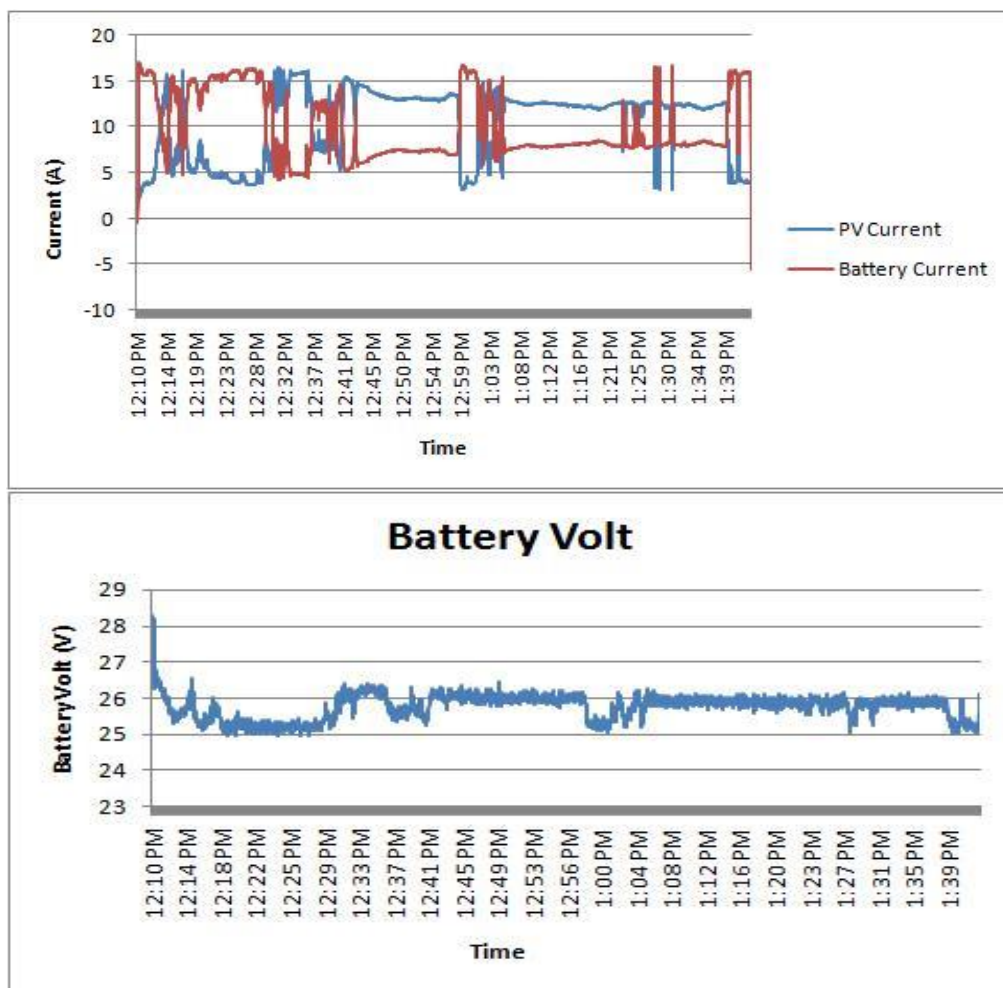
Fig. 13. Battery volt variation when subjected to a constant load (200 watt) and fluctuating PV current (cloudy day)

Rys. 13. Zmiana napięcia akumulatora poddana stałemu obciążeniu (200 watów) i zmiennemu prądowi PV (dzień pochmurny)

## 5.5. Case five: raining day with different loads

The system's performance on a rainy day, during which no *PV* current was generated due to overcast conditions, is illustrated in Figure 16. The data represents a time when the system worked at half load (200 watts) from 12:34 PM to 1:34 PM, followed by a full load (450 watts) from 1:34 PM to 2:05 PM. During the peak load phase, which coincided with the rainfall, the *PV* output was nil, making the system completely reliant on battery power to satisfy load demands.
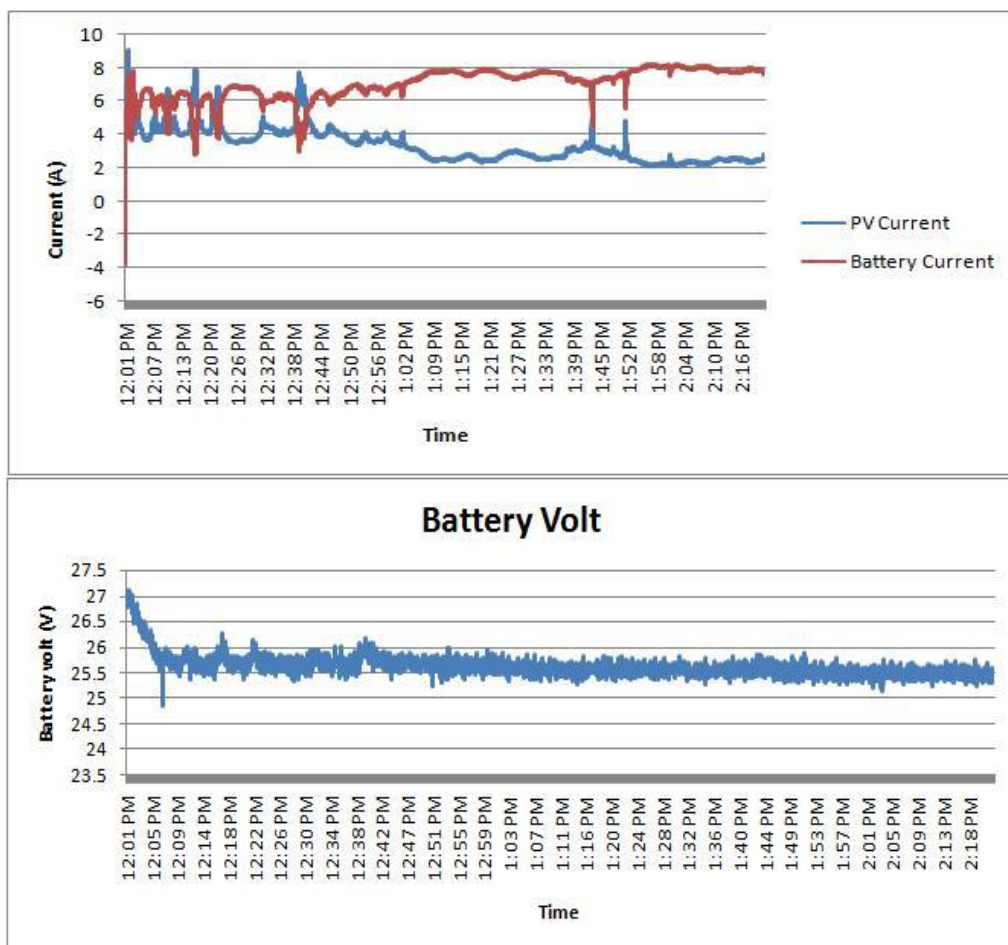
Fig. 14. Minimal fluctuation due to rare sun shine times, initial SOC of this run was 98% and the load was 200 W

Rys. 14. Minimalne wahania spowodowane rzadkim nasłonecznieniem, początkowy SOC tego biegu wynosił 98%, a obciążenie 200 W
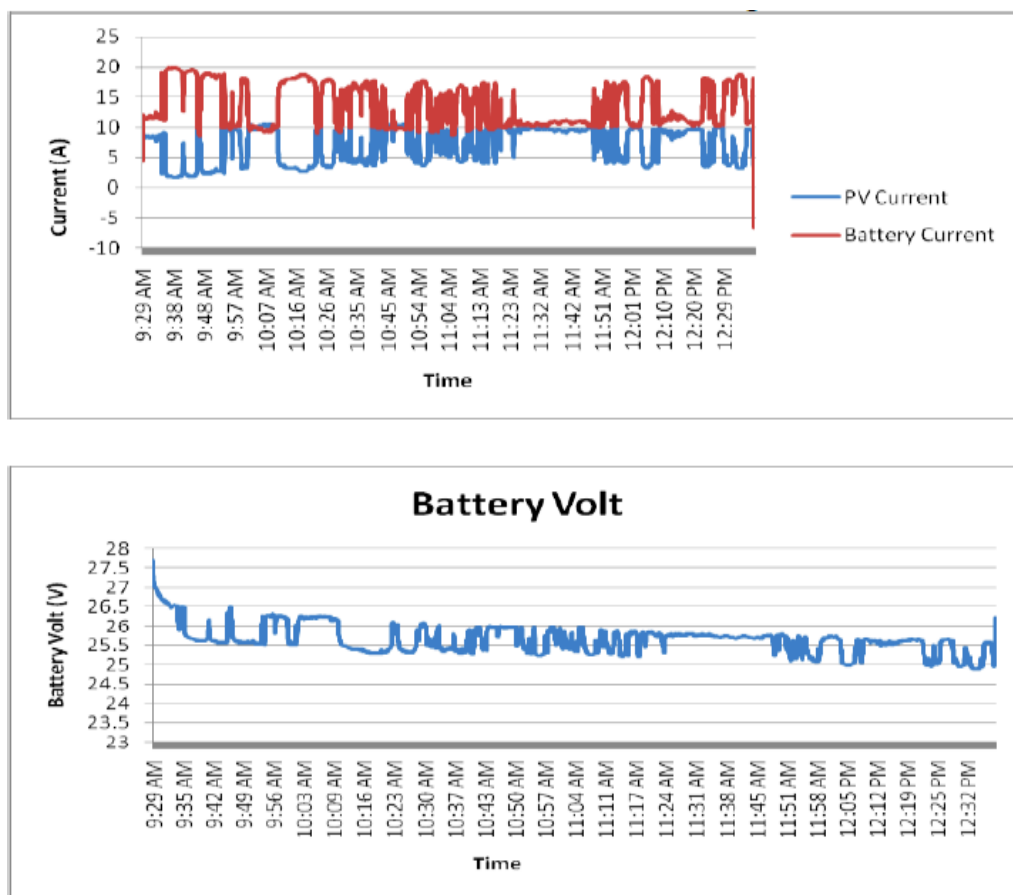
Fig. 15. System performance at cloudy day with fluctuation of sun shines

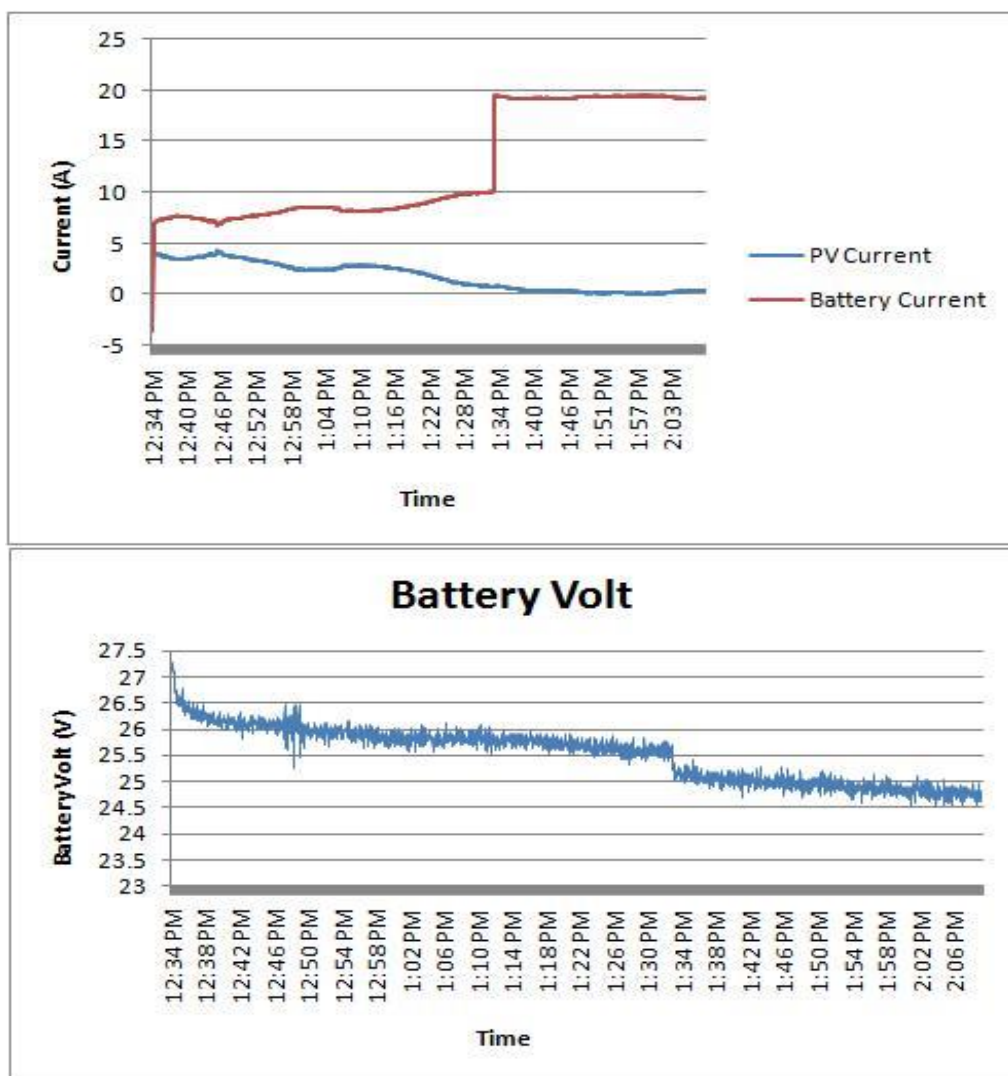Rys. 15. Wydajność systemu w pochmurny dzień z wahaniami nasłonecznienia

Fig. 16. System performance at half load (200 watt) from 12:34 to 1:34 PM and full load from 1:34 to 2:05 PM (450 watt)

Rys. 16. Wydajność systemu przy połowie obciążenia (200 watów) od 12:34 do 1:34 po południu i pełnym obciążeniu od 1:34 do 2:05 po południu (450 watów)

# Conclusions

Renewable energies are gaining popularity due to their low $CO_2$ emissions compared to conventional energy sources, which are known for their significant environmental impact. However, controlling these systems and devising efficient control mechanisms is still a topic of current research. The hybrid renewable energy system described here combines several energy-producing components, such as *PV* modules, storage batteries, and a charge controller, with a diesel generator serving as a backup energy source. It is supplemented by a DC/AC power inverter and a complete control scheme. The control panel includes a USB data acquisition card connected to a PC, as well as several signal conditioning devices and transducers, all of which are controlled by a custom-developed LABVIEW software application. After installation, the device was calibrated to ensure proper functioning operation. The system's performance under both fixed and variable loads was carefully assessed in order to reflect its operational status accurately. Key findings of the study include:

◆ The devised control scheme is efficient for controlling HRES in all operating situations and may apply various control techniques for a standalone *PV* system.

◆ SOC [%] has no significant impact on battery output under varied loads, provided the current demand does not exceed the battery's maximum current.

◆ Higher discharged current leads to a significant decrease in battery usable capacity, indicating poor battery performance.

◆ It is also possible to use the IV-curves to detect the battery state of charge and protect batteries below 35%.

◆ When the *PV* current exceeds the load demand, the excess is sent to the battery, which increases its charge.

◆ The controller successfully detected the requirement for the pack-up generator and performed necessary control operations, including disconnecting the *PV* and battery system and starting the generator.

The Author have no conflicts of interest to declare.

# References

Abd-Elaziz et al. 2021 – Abd-Elaziz, A.A., Dabour, S.M., Elmorshedy, M.F. and Rashad, E.M. 2021. Modeling and control of stand-alone photovoltaic system based on split-source inverter. [In:] *2021 22nd International Middle East Power Systems Conference* (*MEPCON*), IEEE, pp. 469–476, DOI: 10.1109/MEPCON50283.2021.9686249.

Abdelmjid, S.A.K.A. 2020. Techno-economic Assessement of Hybrid Energy System for a Stand-alone Load in Morocco. *International Journal of Renewable Energy Research* (*IJRER*) 10(4), pp. 1774–1782, DOI: 10.20508/ijrer.v10i4.11453.g8067.

Abed et al. 2018 – Abed, K.A., Bahgat, A., Badr, M.A., El-Bayoumi, M. and Ragheb, A.A. 2018. Experimental study of battery state of charge effect on battery charging/discharging performance and battery output power in pv energy system. *ARPN Journal of Engineering and Applied Sciences* 13(2), pp. 739–745.

Belboul et al. 2024 – Belboul, Z., Toual, B., Bensalem, A., Ghenai, C., Khan, B. and Kamel, S. 2024. Techno-economic optimization for isolated hybrid PV/wind/battery/diesel generator microgrid using improved salp swarm algorithm. *Scientific Reports* 14(1), DOI: 10.1038/s41598-024-52232-y.

Bilal et al. 2012 – Bilal, B.O., Sambou, V., Kébé, C.M.F., Ndiaye, P.A. and Ndongo, M. 2012. Methodology to Size an Optimal Stand-Alone PV/wind/diesel/battery System Minimizing the Levelized cost of Energy and the $CO_2$ Emissions. *Energy Procedia* 14, pp. 1636–1647, DOI: 10.1016/j.egypro.2011.12.1145.

Castañeda et al. 2013 – Castañeda, M., Cano, A., Jurado, F., Sánchez, H. and Fernández, L.M. 2013. Sizing optimization, dynamic modeling and energy management strategies of a stand-alone PV/hydrogen/ battery-based hybrid system. *International journal of hydrogen energy* 38(10), pp. 3830–3845, DOI: 10.1016/j.ijhydene.2013.01.080.

Chen, Y. and Zhang, S. 2023. Technical, economic, and environmental assessment of a stand-alone power system based on diesel engine with/without energy storage using an optimization algorithm: A case study in China. *Environmental Science and Pollution Research* 31, pp. 38585–38602, DOI: 10.1007/ s11356-023-31488-3.

Datta et al. 2009 – Datta, M., Senjyu, T., Yona, A., Funabashi, T. and Kim, C.H. 2009. A coordinated control method for leveling PV output power fluctuations of PV–diesel hybrid systems connected to isolated power utility. *IEEE Transactions on Energy Conversion* 24(1), pp. 153–162, DOI: 10.1109/ TEC.2008.2008870.

Datta et al. 2010 – Datta, M.,Senjyu, T., Yona, A., Funabashi, T. and Kim, C.H. 2010. A frequency-control approach by photovoltaic generator in a PV–diesel hybrid power system. *IEEE Transactions on Energy Conversion* 26(2), pp. 559–571, DOI: 10.1109/TEC.2010.2089688.

Deshmukh et al. 2008 – Deshmukh, M.K. and Deshmukh, S.S. 2008. Modeling of hybrid renewable energy systems. *Renewable and sustainable energy reviews* 12(1), pp. 235–249, DOI: 10.1016/j. rser.2006.07.011.

Duryea et al. 1999 – Duryea, S., Islam, S. and Lawrance, W. 1999. A battery management system for stand alone photovoltaic energy systems. [In:] *Conference Record of the 1999 IEEE Industry Applications Conference*. Thirty-Forth IAS Annual Meeting (Cat. No. 99CH36370) 4, pp. 2649–2654, DOI: 10.1109/ IAS.1999.799211.

El-Hefnawi, S.H. 1998. Photovoltaic diesel-generator hybrid power system sizing. *Renewable Energy* 13(1), pp. 33–40, DOI: 10.1016/S0960-1481(97)00074-8.

Farahat et al. 2019 – Farahat, M.A., Abd El-Gawad, Amal F. and Abaza, H.M. 2019. Modeling and Sizing of the Standalone PV with Battery Systems. *Journal of Engineering Research and Application* 9(8) (Series-V), pp. 18–27, DOI: 10.9790/9622- 0908051827.

Ganthia et al. 2022 – Ganthia, B.P., Dharmaprakash, R., Choudhary, T., Muni, T.V., Al-Ammar, E.A., Seikh, A.H. and Diriba, A. 2022. Simulation model of PV system function in stand-alone mode for grid blackout area. *International Journal of Photoenergy*, DOI: 10.1155/2022/6202802.

Gevorgian et al. 2022 – Gevorgian, V., Koralewicz, P., Shah, S., Mendiola, E., Wallen, R. and Villegas Pico, H. 2022. Photovoltaic plant and battery energy storage system integration at NREL's Flatirons campus (No. NREL/TP-5D00-81104). *National Renewable Energy Laboratory* (NREL), Golden, CO (United States), DOI: 10.2172/1846617.

Habib et al. 2019 – Habib, H.U.R., Wang, S., Elkadeem, M.R. and Elmorshedy, M.F. 2019. Design optimization and model predictive control of a standalone hybrid renewable energy system: A case study on a small residential load in Pakistan. *IEEE Access* 7, pp. 117369–117390, DOI: 10.1109/ACCESS.2019.2936789.

Hansen et al. 2001 – Hansen, A.D., Sørensen, P.E., Hansen, L.H. and Bindner, H.W. 2001. *Models for a stand-alone PV system*. Denmark. Forskningscenter Risoe. Risoe-R No. 1219(EN).

Ibrahim, M.I.A.H. 2002. *Decentralized hybrid renewable energy systems: control optimization and battery ageing estimation based on fuzzy logic*. dissertation. de. Ph. D. Thesis, Kassel University, Germany.

Maleki, A. and Pourfayaz, F. 2015. Sizing of stand-alone photovoltaic/wind/diesel system with battery and fuel cell storage devices by harmony search algorithm. *Journal of Energy Storage* 2, pp. 30–42, DOI: 10.1016/j.est.2015.05.006.

Mohanty et al. 2015 – Mohanty, D., Dash, S. and Agarwal, M.S. 2015. Design of Battery Energy Storage System for Generation of Solar Power. *International Journal of Engineering Research & Technology* 4(4), DOI: 10.17577/IJERTV4IS040550.

Nfah et al. 2007 – Nfah, E.M., Ngundam, J.M. and Tchinda, R. 2007. Modelling of solar/diesel/battery hybrid power systems for far-north Cameroon. *Renewable Energy* 32(5), pp. 832–844, DOI: 10.1016/j.renene.2006.03.010.

Ramli et al. 2015 – Ramli, M.A., Hiendro, A. and Twaha, S. 2015. Economic analysis of PV/diesel hybrid system with flywheel energy storage. *Renewable Energy* 78, pp. 398–405, DOI: 10.1016/j.renene.2015.01.026.

Saib et al. 2024 – Saib, S., Bayındır, R. and Vadi, S. 2024. Overview: Using Hybrid Energy System for Electricity Production Based on the Optimization Methods. *Gazi University Journal of Science* 37(2), pp. 745–772, DOI: 10.35378/gujs.1328300.

Shaahid, S.M. and Elhadidy, M.A. 2008. Economic analysis of hybrid photovoltaic–diesel–battery power systems for residential loads in hot regions – A step to clean future. *Renewable and sustainable energy reviews* 12(2), pp. 488–503, DOI: 10.1016/j.rser.2006.07.013.

Shen, W.X. 2009. Optimally sizing of solar array and battery in a standalone photovoltaic system in Malaysia. *Renewable energy* 34(1), pp. 348–352, DOI: 10.1016/j.renene.2008.03.015.

Shin et al. 2015 – Shin, Y., Koo, W.Y., Kim, T.H., Jung, S. and Kim, H. 2015. Capacity design and operation planning of a hybrid PV–wind–battery–diesel power generation system in the case of Deokjeok Island. *Applied Thermal Engineering* 89, pp. 514–525, DOI: 10.1016/j.applthermaleng.2015.06.043.

Thirunavukkarasu et al. 2020 – Thirunavukkarasu, M. and Sawle, Y. 2020. Design, analysis and optimal sizing of standalone PV/diesel/battery hybrid energy system using HOMER. [In:] *IOP conference series: materials science and engineering* 937(1), IOP Publishing, DOI: 10.1088/1757-899X/937/1/012034.

Yap, W.K. and Karri, V. 2015. An off-grid hybrid PV/diesel model as a planning and design tool, incorporating dynamic and ANN modelling techniques. *Renewable Energy* 78, pp. 42–50, DOI: 10.1016/j.renene.2014.12.065.

Zhang et al. 2017 – Zhang, J., Huang, L., Shu, J., Wang, H. and Ding, J. 2017. Energy management of PV-diesel-battery hybrid power system for island stand-alone micro-grid. *Energy Procedia* 105, pp. 2201–2206, DOI: 10.1016/j.egypro.2017.03.622.

Zhou et al. 2010 – Zhou, W., Lou, C., Li, Z., Lu, L. and Yang, H. 2010. Current status of research on optimum sizing of stand-alone hybrid solar–wind power generation systems. *Applied energy* 87(2), pp. 380–389, DOI: 10.1016/j.apenergy.2009.08.012.

Mubarak ALANAZI

# Kontrola i monitorowanie autonomicznych hybrydowych systemów energii odnawialnej

## Streszczenie

Magazynowanie energii odgrywa kluczową rolę w autonomicznych hybrydowych systemach energii odnawialnej, zapewniając stabilne i niezawodne zasilanie na obszarach wiejskich odłączonych od sieci elektrycznej. W niniejszym artykule zintegrowano akumulatory i zapasowy generator diesla w celu utrzymania ciągłej dostępności energii. Komputerowa jednostka monitorująca i sterująca została opracowana w celu optymalizacji wydajności systemu, zwiększenia efektywności i poprawy zrównoważonego rozwoju. Układ eksperymentalny składa się z paneli fotowoltaicznych (PV), generatora diesla (DG), baterii akumulatorów (B), kontrolera ładowania, falownika DC/AC i zmiennego obciążenia elektrycznego. Jednostka sterująca, zaprojektowana przy użyciu oprogramowania LabView, zapobiega nadmiernemu rozładowaniu akumulatora, poprawiając w ten sposób jego żywotność i ogólną wydajność. Składa się z czujników napięcia i prądu podłączonych do kart akwizycji danych (DAC) połączonych z komputerem PC. System obejmuje dwanaście paneli fotowoltaicznych 12 V, każdy o mocy 75 W, dostarczających łącznie 450 W. Wyniki eksperymentów wskazują, że pojemność baterii znacznie spada przy wysokich prądach rozładowania, co podkreśla konieczność stosowania skutecznych strategii zarządzania energią. Jednostka sterująca stale monitoruje parametry systemu i reguluje działanie generatora zapasowego. Gdy stan naładowania akumulatora (SOC) spada do 35%, system automatycznie odłącza obciążenie i aktywuje DG, zapewniając nieprzerwane zasilanie przy jednoczesnym przedłużeniu żywotności akumulatora. Wyniki te podkreślają znaczenie wyboru odpowiednich rozmiarów i charakterystyk baterii, biorąc pod uwagę zarówno koszty, jak i wymagania dotyczące obciążenia, w celu zwiększenia wydajności, niezawodności i ekonomicznej wykonalności hybrydowych systemów energii odnawialnej do zastosowań poza siecią.

SŁOWA KLUCZOWE: energia odnawialna, akumulatory, system kontroli i monitorowania energii, magazynowanie energii